

Hydrogen-Bonding and Ion–Ion Interactions in Solutions of Triflic Acid and 1-Ethyl-3-methylimidazolium Triflate

Christopher M. Burba,^{*,†} Nathalie M. Rocher,[‡] and Roger Frech[§]

Department of Natural Sciences, Northeastern State University, Tahlequah, Oklahoma 74464-2302, Department of Materials Engineering, Monash University, Clayton, Victoria 3800 Australia, and Department of Chemistry and Biochemistry, University of Oklahoma, Norman, Oklahoma 73019-3051

Received: March 13, 2009; Revised Manuscript Received: June 23, 2009

Ion–ion and hydrogen-bonding interactions in solutions of 1-ethyl-3-methylimidazolium trifluoromethanesulfonate ([C₂mim]Tf) and triflic acid (HTf) are investigated with infrared and Raman spectroscopy. Bands indicative of highly aggregated triflate anions appear in the vibrational spectra of solutions containing a large fraction of triflic acid. These species most likely consist of triflate anions that are at least threefold coordinated by positive ions (i.e., {[C₂mim]_xH_yTf}^{x+y−1} where $x + y \geq 3$). Such coordination environments would be consistent with a larger, extended aggregate of Tf[−], [C₂mim]⁺, and H⁺ ions that may be charged or neutral. Evidence for hydrogen bonding between the protons and the oxygen atoms of the triflate anions and between the hydrogen atoms of the [C₂mim]⁺ and triflate anion is identified in the infrared and Raman spectra.

1. Introduction

Room-temperature ionic liquids (RTILs) hold tremendous promise as solvent systems for a wide variety of applications. Most RTILs consist of bulky ions that possess highly delocalized charges, and the resulting low lattice energies permit the salts to exist in a molten state at ambient temperatures. To a large degree, the success of RTILs hinges on the low vapor pressures, low flammabilities, and high ionic conductivities of the compounds. In addition, the synthetic versatility available in designing constituent ions allows researchers to modify other key solvent properties of the ionic liquid, such as degree of hydrophobicity or hydrophilicity, viscosity, conductivity, and electrochemical window. Thus, an ionic liquid can be tailored to the needs of a particular application.

One potential use of RTILs is to boost the poor high-temperature performance of proton-exchange membrane (PEM) fuel cells. To date, most PEM fuel cells are based on fluorinated sulfonic acid polymers such as Nafion and Aciplex.¹ These compounds deliver excellent proton conductivities when hydrated, but exhibit poorer performance when the temperature exceeds 100 °C and the polymer dehydrates. Unfortunately, the platinum catalysts used in a fuel cell are more susceptible to poisoning at low temperatures;² hence, there is an impetus to prepare new PEMs that are robust to temperatures higher than 100 °C. Ionic liquid-doped polymer films have been suggested as a potential solution to the poor high-temperature performance of traditional fuel cell membranes. Proton-exchange membranes doped with a RTIL might retain high conductivities at elevated temperatures, thereby offering an attractive approach toward improved performance.^{3–5} For example, Doyle and co-workers impregnated a Nafion membrane with 1-butyl-3-methylimidazolium trifluoromethanesulfonate, an aprotic ionic liquid, and the resulting PEM delivered conductivities near 0.1 S·cm^{−1} at 180 °C.⁶ It is possible that higher proton conductivities may be

achieved by doping a PEM with an ionic liquid along with a superacid, such as trifluoromethanesulfonic acid.

To some degree, the conductivity of a PEM is influenced by ion–ion interactions. Systems containing an abundance of neutral ion pairs or low-mobility aggregates often yield low conductivities and poor performance.⁷ Therefore, a key step in developing ionic liquid-based PEMs is to understand how the individual components interact with one another on a molecular level. Undoubtedly, the interactions between the ionic liquid, superacid, and polymer host will be very complicated. A good first step toward unraveling the molecular-level interactions in these types of systems is exploring binary combinations of the individual components. In this report, ion–ion interactions will be investigated for solutions of 1-ethyl-3-methylimidazolium trifluoromethanesulfonate and trifluoromethanesulfonic acid. Both components are important candidates for fuel cell applications, and these studies will provide a good starting point for examining the interactions of more complicated, tertiary PEMs involving an ionic liquid, superacid, and polymer.

2. Experimental Methods

2.1. Materials. Trifluoromethanesulfonic acid (hereafter, “triflic acid” or HTf), and 1-ethyl-3-methylimidazolium trifluoromethanesulfonate ([C₂mim]Tf) were purchased from Aldrich and used as received. Both compounds were stored and manipulated under an argon atmosphere (≤1 ppm H₂O). Solutions were prepared by mixing appropriate masses of each precursor, and each solution was stirred for a minimum of 24 h prior to spectroscopic analysis. Compositions are reported as mole ratios of [C₂mim]Tf and HTf, [C₂mim]Tf:HTf. Spectral deconvolution was accomplished with Galatic Grams AI.

2.2. Vibrational Spectroscopy. Infrared absorption spectra were collected using a Brüker IFS 66v Fourier transform infrared spectrometer (KBr beam splitter and DTGS detector). Samples were placed between two ZnSe windows and spectra were measured under dry air purge at 1 cm^{−1} resolution. FT-Raman spectroscopy was performed with a FRA 106/S mounted on a Brüker Equinox 55 spectrometer. Samples were sealed inside thin-walled, quartz NMR tubes under an argon atmosphere. The

* Corresponding author. E-mail: burba@nsuok.edu.

[†] Northeastern State University.

[‡] Monash University.

[§] University of Oklahoma.

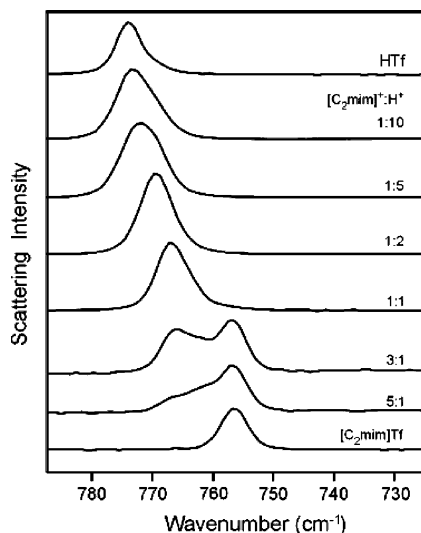


Figure 1. Raman scattering spectra showing the $\delta_s(\text{CF}_3)$ modes of the triflate anion for several different $[\text{C}_2\text{mim}]\text{Tf}$ –HTf solution compositions. Compositions are noted in the figure.

1064 nm line of a Nd:YAG laser was used as the excitation source, and the data were recorded at 2 cm^{-1} resolution.

3. Results

3.1. Vibrational Modes of the Triflate Anions. The local environment surrounding the triflate anions in the $[\text{C}_2\text{mim}]\text{Tf}$ –HTf solutions is investigated by monitoring two vibrational modes of the triflate anion: the CF_3 symmetric deformation, $\delta_s(\text{CF}_3)$, and the SO_3 symmetric stretching motion, $\nu_s(\text{SO}_3)$. These vibrational modes are known to be very sensitive to the coordination environment of a triflate anion and provide information concerning ion–ion interactions in the $[\text{C}_2\text{mim}]\text{Tf}$ –HTf solutions from the perspective of the anions.

Figure 1 depicts Raman spectra of solutions between 800 and 725 cm^{-1} . Pure $[\text{C}_2\text{mim}]\text{Tf}$ contains a single $\delta_s(\text{CF}_3)$ band at 757 cm^{-1} . No significant changes in the Raman spectra are detected for dilute solutions of triflic acid in the ionic liquid ($[\text{C}_2\text{mim}]\text{Tf}$:HTf mole ratios up to 10:1); however, a new band appears at 766 cm^{-1} in the Raman spectrum of the 5:1 sample and increases in intensity at the expense of the 757 cm^{-1} band as the relative amount of HTf is increased. The 757 cm^{-1} band is completely absent from the Raman spectrum of the 1:1 sample, leaving only the 766 cm^{-1} band. Increased addition of triflic acid causes the frequency of the 766 cm^{-1} band to gradually shift to 773 cm^{-1} .

Infrared spectra of the $[\text{C}_2\text{mim}]\text{Tf}$ –HTf solutions are presented in Figure 2. The $\delta_s(\text{CF}_3)$ mode of pure $[\text{C}_2\text{mim}]\text{Tf}$ occurs at 757 cm^{-1} , consistent with the Raman spectrum of $[\text{C}_2\text{mim}]\text{Tf}$ in Figure 1. The $\delta_s(\text{CF}_3)$ band is partially obscured by a very broad $[\text{C}_2\text{mim}]^+$ band near 757 cm^{-1} that Talaty and co-workers assign to HCCH bending motions of the imidazolium ring.⁸ This $[\text{C}_2\text{mim}]^+$ mode shifts to slightly lower frequencies in triflic acid-rich solutions (see Figure 2). Although the $\delta_s(\text{CF}_3)$ band is partially obscured by the $[\text{C}_2\text{mim}]^+$ band, the infrared spectra of $[\text{C}_2\text{mim}]\text{Tf}$ –HTf solutions exhibit trends similar to those of the corresponding Raman spectra shown in Figure 1. For instance, a new band at 766 cm^{-1} grows in intensity and eventually replaces the 757 cm^{-1} band as the solution composition is increased to 1:1. The frequency of the 766 cm^{-1} band then increases as the composition of the solutions approaches pure triflic acid.

Raman and infrared spectra of the $\nu_s(\text{SO}_3)$ bands of the $[\text{C}_2\text{mim}]\text{Tf}$ –HTf solutions are provided in Figures 3 and 4,

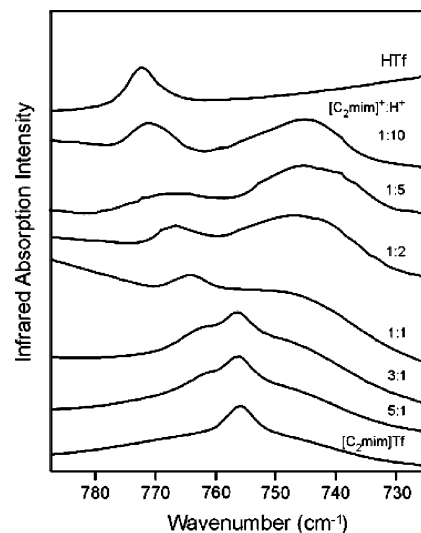


Figure 2. Infrared absorption spectra illustrating the $\delta_s(\text{CF}_3)$ modes of the triflate anion for several different $[\text{C}_2\text{mim}]\text{Tf}$ –HTf solution compositions. Compositions are noted in the figure.

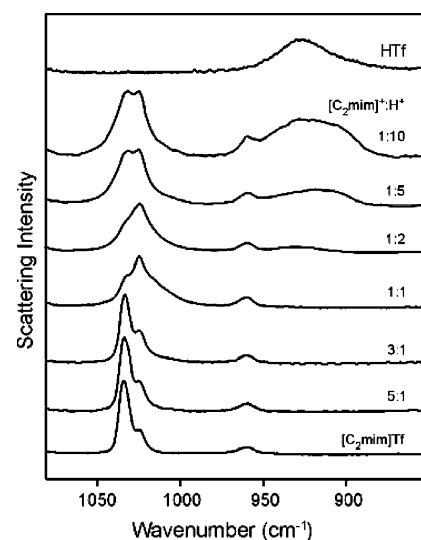


Figure 3. Raman scattering spectra of the $\nu_s(\text{SO}_3)$ modes of the triflate anion for several different $[\text{C}_2\text{mim}]\text{Tf}$ –HTf solution compositions. Compositions are noted in the figure.

respectively. The Raman spectrum of the pure ionic liquid contains a single $\nu_s(\text{SO}_3)$ band at 1032 cm^{-1} along with bands that may be attributed to the $[\text{C}_2\text{mim}]^+$ cations at 1025 and 960 cm^{-1} .⁸ The $\nu_s(\text{SO}_3)$ band gradually decreases in intensity and broadens as triflic acid is added to the ionic liquid, until the Raman spectrum of the 1:1 sample is dominated by the 1025 cm^{-1} band. In triflic acid-rich solutions, the 1032 cm^{-1} band increases in intensity relative to the 1025 cm^{-1} band and a new broad band begins to appear near 925 cm^{-1} that also increases in intensity and significantly broadens. The Raman spectrum of pure triflic acid is characterized by a very broad band roughly centered at 925 cm^{-1} , but lacks the spectroscopic features near 1030 cm^{-1} that are observed in the $[\text{C}_2\text{mim}]\text{Tf}$ –HTf solutions.

Infrared spectra of the $\nu_s(\text{SO}_3)$ bands follow the same general trends as the Raman spectra (Figure 4). The spectrum of pure $[\text{C}_2\text{mim}]\text{Tf}$ consists of several overlapping features centered at roughly 1030 cm^{-1} with an additional weak band at 1017 cm^{-1} that is assigned as a vibration of the $[\text{C}_2\text{mim}]^+$ cations.⁸ The $\nu_s(\text{SO}_3)$ band somewhat narrows when HTf is added to the ionic liquid. In triflic acid-rich solutions, $\nu_s(\text{SO}_3)$ bands occur near

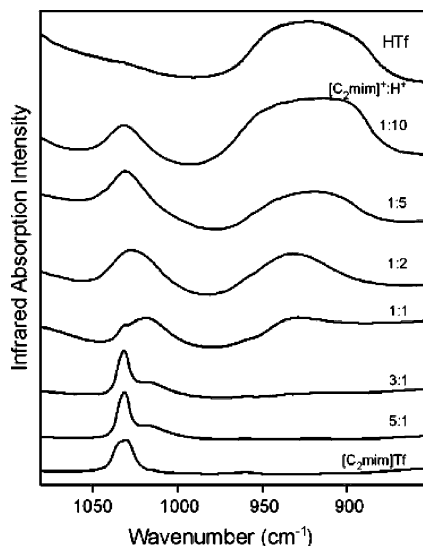


Figure 4. Infrared absorption spectra showing the $\nu_s(\text{SO}_3)$ modes of the triflate anion for several different $[\text{C}_2\text{mim}]\text{Tf}$ –HTf solution compositions. Compositions are noted in the figure.

1030 cm^{-1} while a new broad band roughly centered at 925 cm^{-1} appears. Band assignments for the vibrational modes of triflic acid have been reported in the literature and are adopted here.^{9–11} On the basis of those studies, the 925 cm^{-1} band is assigned to vibrations of S–OH groups of the triflate anions.

3.2. Vibrational Modes of the $[\text{C}_2\text{mim}]^+$ Cations. The vibrational modes of the $[\text{C}_2\text{mim}]^+$ ion have been examined by several research groups.^{8,12,13} The ethyl group of the $[\text{C}_2\text{mim}]^+$ cation may adopt either a planar or a nonplanar conformation with respect to the imidazolium ring. Umehayashi and co-workers¹² used quantum chemical calculations to show that there is a slight energy difference between the two possible conformations. Early Raman scattering experiments demonstrated that low-frequency imidazolium ion vibrations (e.g., bands between 500 and 200 cm^{-1}) are sensitive to the two conformations and may be used to probe the conformational equilibrium.¹² Las-sègues and colleagues¹³ later expanded these studies to include solutions of lithium salts dissolved in a $[\text{C}_2\text{mim}]$ -based ionic liquid. Low-frequency Raman spectra are examined for the $[\text{C}_2\text{mim}]\text{Tf}$ –HTf solutions. The low-frequency bands of the solutions appear very similar to those of the pure ionic liquid, possibly indicating that triflic acid has a minimal impact on the conformational equilibrium of the $[\text{C}_2\text{mim}]^+$ ions. However, the overlapping bands from the triflate anion—along with the very weak intensities of the $[\text{C}_2\text{mim}]^+$ bands in the triflic acid-rich solutions—made spectral deconvolution difficult. The low-frequency Raman spectra are not shown since the spectra are very similar to those of pure $[\text{C}_2\text{mim}]\text{Tf}$ shown in ref 12.

Figure 5 illustrates spectral changes in the C–H stretching bands of the $[\text{C}_2\text{mim}]^+$ cation for the $[\text{C}_2\text{mim}]\text{Tf}$ –HTf solution series. The dashed lines on the figure mark several bands that are thought to be sensitive to hydrogen-bonding interactions of the $[\text{C}_2\text{mim}]^+$ cations.⁸ Most of the C–H bands shown in Figure 5 shift to higher frequencies when triflic acid is added to $[\text{C}_2\text{mim}]\text{Tf}$. Some of the bands undergo slight changes (e.g., 2969 to 2971 cm^{-1}), whereas other changes are more dramatic (viz., 3169 to 3183 cm^{-1}). The Raman spectrum of pure triflic acid lacks spectral features at these frequencies and is thus not shown. Other regions of the spectrum contain vibrational modes of the $[\text{C}_2\text{mim}]^+$ cation; however, very few changes are observed in the frequencies or relative intensities of those bands.

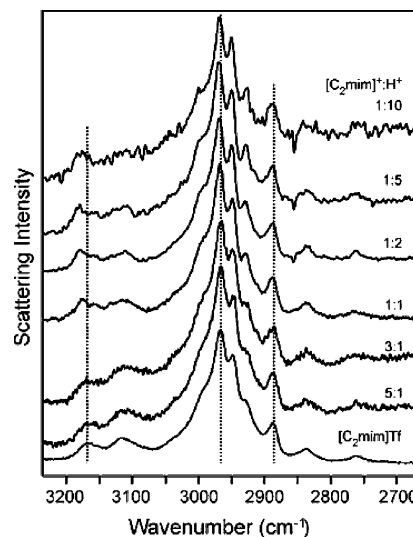


Figure 5. Raman scattering spectra depicting the C–H stretching modes of several different $[\text{C}_2\text{mim}]\text{Tf}$ –HTf solutions. Compositions are noted in the figure.

4. Discussion

4.1. Speciation of the Triflate Anions. The frequencies and intensities of the vibrational modes for the triflate anions undergo significant changes when triflic acid is added to $[\text{C}_2\text{mim}]\text{Tf}$. The small size and high charge density of a proton compared to a bulky $[\text{C}_2\text{mim}]^+$ cation facilitates strong interactions with the oxygen atoms of the triflate molecule, possibly leading to the formation of neutral contact ion pairs or higher order aggregates such as $[\text{H}_2\text{Tf}]^+$ or $[\text{HTf}_2]^-$. The electron distribution within a triflate anion participating in an aggregate species is expected to be different from anions that are exclusively coordinated by $[\text{C}_2\text{mim}]^+$ cations, thereby affecting the force constants (vibrational band frequencies), polarizability derivatives (Raman band intensities), and dipole moment derivatives (infrared band intensities) of the triflate anion. Consequently, the vibrational spectroscopic signature of protonated triflate anions will be distinctly different from that of triflate anions that are coordinated only by $[\text{C}_2\text{mim}]^+$ cations. The integrated intensity of the infrared- and Raman-active modes of the various chemical species present in a solution is proportional to the relative concentration of those species. Thus, infrared and Raman spectra of $[\text{C}_2\text{mim}]\text{Tf}$ –HTf solutions can provide some insight into the fraction of triflate anions that are involved in each coordination environment.

At low mole ratios ($[\text{C}_2\text{mim}]\text{Tf}:\text{HTf} < 5:1$), the vibrational spectrum resembles that of pure $[\text{C}_2\text{mim}]\text{Tf}$. In these solutions, the triflate anions are coordinated predominantly by $[\text{C}_2\text{mim}]^+$ cations, yielding a single $\delta_s(\text{CF}_3)$ band at 757 cm^{-1} and $\nu_s(\text{SO}_3)$ bands in the vicinity of 1032 cm^{-1} in the Raman and IR spectra. The frequency of the 1032 cm^{-1} band is consistent with “free” triflate anions. Previous spectroscopic¹⁴ and computational^{14,15} investigations indicate that the $\delta_s(\text{CF}_3)$ mode for “free” triflate anions occurs at 753 – 754 cm^{-1} , whereas ion-paired species (specifically $\text{Li}^+\cdots\text{Tf}^-$ ion pairs) have $\delta_s(\text{CF}_3)$ bands at 756 cm^{-1} . Higher frequencies have been reported for aggregated triflate ions. These assignments are supported by a combination of single-crystal X-ray crystallographic and vibrational spectroscopic studies in which ion-paired triflate anions have $\delta_s(\text{CF}_3)$ band frequencies near 756 cm^{-1} .^{16–20} The apparent discrepancy in the coordination environment of the triflate anions, as measured from frequency shifts of the $\nu_s(\text{SO}_3)$ and $\delta_s(\text{CF}_3)$ bands, has been observed in other systems involving Li^+

TABLE 1: Spectral Curve-Fitting Results for the $\delta_s(\text{CF}_3)$ Bands from the Raman Spectra of the $[\text{C}_2\text{mim}]\text{Tf}-\text{HTf}$ Solutions^a

frequency (cm^{-1})	solution composition (mole ratio, $[\text{C}_2\text{mim}]\text{Tf}:\text{HTf}$)								
	$[\text{C}_2\text{mim}]\text{Tf}$	10:1	5:1	3:1	1:1	1:2	1:5	1:10	HTf
757	100.0	70.0	61.8	43.5	4.0				
762		30.0	20.9	23.3	6.2				
767			17.3	33.2	89.8	9.8			
769						90.2	49.3	34.3	11.8
774							50.7	65.7	88.2

^a Data are reported as the percentage of each band observed at a given composition.

coordination with hydrogen bonding present.^{21,22} In those studies, the $\delta_s(\text{CF}_3)$ band gives the “correct” frequency for ion-paired species, while $\nu_s(\text{SO}_3)$ gives the “incorrect” free-ion frequency. In this paper, we are discussing hydrogen-bonding interactions or even protonation and also interactions between Tf^- and the $[\text{C}_2\text{mim}]^+$ cations. Thus, it is not surprising that the frequency of the $\nu_s(\text{SO}_3)$ band is consistent with “free” ions, whereas the $\delta_s(\text{CF}_3)$ band frequency suggests ion-paired triflate anions. We assign the 757 cm^{-1} band of pure $[\text{C}_2\text{mim}]\text{Tf}$ and low mole ratio solutions to triflate ions that are coordinated solely by $[\text{C}_2\text{mim}]^+$ ions. This assignment is further supported by Raman spectroscopic studies of poly(ethylene oxide), PEO, doped with $[\text{C}_2\text{mim}]\text{Tf}$.²³ In that system, the frequency of the $\delta_s(\text{CF}_3)$ band falls to 754 cm^{-1} when the ether oxygen to $[\text{C}_2\text{mim}]\text{Tf}$ ratio is less than 20:1 ($\text{O}:[\text{C}_2\text{mim}]^+$). The lower frequency of the $\delta_s(\text{CF}_3)$ band suggests that PEO effectively dissociates the ionic liquid at low compositions, producing “free” triflate anions.

Choudhury and co-workers used X-ray diffraction methods on $[\text{C}_2\text{mim}]\text{Tf}$ single crystals to reveal hydrogen-bonding interactions between hydrogen atoms from the imidazolium ring and the oxygen atoms of the triflate anion.²⁴ Similar interactions might exist in the molten state, accounting for the high $\delta_s(\text{CF}_3)$ band frequency for the pure ionic liquid. Another possible interpretation is that the $[\text{C}_2\text{mim}]^+$ ions are not formally coordinated to a specific triflate anion through hydrogen-bonding effects to form a contact ion pair, but perturb the anions through Coulombic interactions. In this scenario, the lifetime of any $[\text{C}_2\text{mim}]^+\cdots\text{Tf}^-$ contact ion pairs that form in the solutions are very short compared to the time scale used in these spectroscopic studies (i.e., less than the time required to complete a few vibrational oscillations). The mere presence of charged ions in the immediate solvation shell around the triflate anions might be sufficient to shift the $\delta_s(\text{CF}_3)$ band to 757 cm^{-1} . In either scenario, the triflate anions in the $[\text{C}_2\text{mim}]\text{Tf}$ ionic liquid are significantly perturbed compared to “free” triflate anions in solutions made from inorganic triflate salts dissolved in neutral solvents.

There are marked changes in the IR and Raman spectra when the composition of the solutions is larger than $[\text{C}_2\text{mim}]\text{Tf}:\text{HTf} = 10:1$. Changes in the frequencies and relative intensities of the $\delta_s(\text{CF}_3)$ and $\nu_s(\text{SO}_3)$ bands for those solutions raise important questions concerning the speciation of the triflate anions. Curve fitting of the $\delta_s(\text{CF}_3)$ bands as a function of triflic acid content are performed to gain a deeper understanding into the speciation and relative concentrations of the triflate anion; such studies are summarized in Table 1. The analysis is only performed on the Raman spectra since the infrared spectra are confounded by overlapping $[\text{C}_2\text{mim}]^+$ vibrations. The appearance of new bands for higher composition solutions signal the presence of triflate anions with different local structures or in different local

environments compared to those in pure $[\text{C}_2\text{mim}]\text{Tf}$. Three overlapped bands are detected in the Raman spectra of the $[\text{C}_2\text{mim}]\text{Tf}-\text{HTf}$ solutions between 10:1 and 1:1. These bands exhibit clear intensity variations as triflic acid is progressively added to the ionic liquid, yet the frequencies of the bands remain unaffected. This behavior points to an equilibrium between three different triflate anion populations in the $[\text{C}_2\text{mim}]\text{Tf}$ -rich solutions. The first population is comprised of triflate anions that have a coordination environment very similar to that of pure $[\text{C}_2\text{mim}]\text{Tf}$, giving rise to a $\delta_s(\text{CF}_3)$ band at 757 cm^{-1} . The second and third populations of triflate anions have $\delta_s(\text{CF}_3)$ bands near 762 and 767 cm^{-1} and most likely consist of protonated triflate anions. The third population of triflate anions—corresponding to the 767 cm^{-1} band—accounts for 17% of the triflate anions in the 5:1 solution. However, equimolar compositions contain a very large number of triflate anions that have a $\delta_s(\text{CF}_3)$ band frequency of 767 cm^{-1} (89.8%). Bands reminiscent of triflate anions coordinated solely by $[\text{C}_2\text{mim}]^+$ ions constitute only 4% of the anions in the 1:1 solution, and the species responsible for the 762 cm^{-1} band makes up 6.2% of the anions. The $[\text{C}_2\text{mim}]\text{Tf}:\text{HTf} = 1:2$ solution consists of two triflate anion populations. Approximately 10% of the anions have $\delta_s(\text{CF}_3)$ band frequencies at 767 cm^{-1} , whereas a new band at 769 cm^{-1} accounts for the remainder of the anions. In solutions with very high triflic acid contents, the 769 cm^{-1} band gradually diminishes as the 774 cm^{-1} band appears. However, the 769 cm^{-1} band is observed in Raman spectrum of pure triflic acid.

It is not immediately clear what triflate-containing species are responsible for the $\delta_s(\text{CF}_3)$ bands at 762 , 767 , or 769 cm^{-1} . Nonetheless, the stoichiometries of the 1:1 and 1:2 solutions along with the presence of dominant bands in the Raman spectra might eliminate some possibilities for the bands at 767 and 769 cm^{-1} . For example, if the 767 cm^{-1} band is attributed to either neutral ion pairs or species such as $[\text{H}_2\text{Tf}]^+$ or H_2Tf_2 , then a large fraction of triflate molecules interacting only with $[\text{C}_2\text{mim}]^+$ cations should be present in the solution. The 757 and 762 cm^{-1} bands represent a small proportion of the triflate anions in the 1:1 solution, and the absence of significant intensities for those bands makes such assignments tenuous. On the basis of the stoichiometry of the solutions, it is possible that the 767 cm^{-1} band is due to $[\text{HTf}_2]^-$ or $[\text{C}_2\text{mim}]\text{HTf}_2$ moieties. Strong interactions between $[\text{C}_2\text{mim}]^+$ and $[\text{HTf}_2]^-$ ions would result in the $\text{H}[\text{C}_2\text{mim}]\text{Tf}_2$ configuration. However, discrete $[\text{HTf}_2]^-$ entities would be expected if the interactions between $[\text{C}_2\text{mim}]^+$ and $[\text{HTf}_2]^-$ are weak. In the latter scenario, the $[\text{C}_2\text{mim}]^+$ ions merely serve to balance the charge of the $[\text{HTf}_2]^-$ anions and do not directly participate in the aggregate species. Similar arguments could be used to assign the 769 cm^{-1} band to $[\text{H}_2\text{Tf}_3]^-$ or $[\text{C}_2\text{mim}]\text{H}_2\text{Tf}_3$ species. Campbell and co-workers²⁵ reported similar anion speciation in solutions of $[\text{C}_2\text{mim}]\text{Cl}$ and HCl using infrared spectroscopy, and Bhargava and Balasubramanian²⁶ used molecular dynamic simulations to identify $[\text{H}_n\text{F}_{n+1}]^-$ species in the $[\text{C}_2\text{mim}]\text{F}-\text{HF}$ system. However, the high frequencies of the 762 , 767 , and 769 cm^{-1} bands are somewhat inconsistent with the relatively low coordination environments of the triflate anions proposed in the above coordination schemes. It is much more likely that these bands are due to highly aggregated triflate anions that are at least threefold coordinated by positive ions (i.e., $\{[\text{C}_2\text{mim}]_x\text{H}_y\text{Tf}\}^{x+y-1}$ where $x + y \geq 3$). Furthermore, such coordination can occur as part of a larger, extended aggregate that may be charged or neutral.

4.2. Hydrogen-Bonding Interactions. Two classes of hydrogen-bonding interactions should be considered for the $[\text{C}_2\text{mim}]\text{Tf}-\text{HTf}$ solutions. The first consists of interactions between protons and the oxygen atoms of the triflate anions, similar to what is found in pure triflic acid. Extensive hydrogen-bonding networks are expected to exist in pure triflic acid and also solutions that contain a high abundance of triflic acid. In contrast, the second class is characterized by hydrogen bonding between hydrogen atoms of the $[\text{C}_2\text{mim}]^+$ ions and the triflate anions. The spectroscopic changes for solutions rich in triflic acid (Figures 1–4) are consistent with the appearance of hydrogen-bonded triflate anions. Evidence for the growth of hydrogen-bonding networks that mimic pure triflic acid is reflected in the spectroscopic data, especially the infrared spectra of the solutions. The appearance of S–OH stretching modes near 925 cm^{-1} and the growth of intense O–H stretching bands in the infrared spectra provide strong evidence for the existence of hydrogen-bonded triflate anion networks in the solutions. Compositions having less triflic acid than the equimolar solution lack these spectral signatures, indicating fewer hydrogen-bonding interactions. Therefore, the immediate interpretation is that the $[\text{C}_2\text{mim}]^+$ ions disrupt hydrogen-bonding interactions, promoting the formation of discrete triflic acid aggregates. Larger clusters of protons and triflate anions (i.e., $[\text{H}_n\text{Tf}_{n+1}]^-$ for $n > 3$) are expected to occur in triflic acid-rich solutions. At those compositions, there will be a deficit of $[\text{C}_2\text{mim}]^+$ ions, allowing some of the aggregated triflate species to coalesce into a network similar to what is expected in pure triflic acid.

There is a growing body of evidence that suggests ion–ion interactions between $[\text{C}_2\text{mim}]^+$ cations and its counterion primarily occurs through a hydrogen atom covalently bonded to the carbon atom that is located between the two nitrogen atoms of the imidazolium ring.^{27–32} These interactions are commonly described as “hydrogen bonds” between the $[\text{C}_2\text{mim}]^+$ cation and the counterion. Computational studies by Talaty and co-workers⁸ suggest that “the Raman C–H stretching band in the vicinity of 3179 cm^{-1} has some potential for studies of hydrogen bonding involving the imidazolium cation.” This band involves motion of the hydrogen atom that is thought to participate in the hydrogen bonds. In pure $[\text{C}_2\text{mim}]\text{Tf}$, this band occurs at 3169 cm^{-1} and increases to 3183 cm^{-1} in triflic acid-rich solutions. The increase in frequency may indicate a change in the strength of the hydrogen bonds formed between the imidazolium cations and the triflate anions as triflic acid is added to the solutions.

Strong hydrogen-bonding interactions between the $[\text{C}_2\text{mim}]^+$ cation and the triflate anion is expected to withdraw electron density from the C–H bond, thereby reducing the force constant of the bond and lowering the C–H stretching frequency. As depicted in Figure 5, solutions containing a high fraction of triflic acid exhibit higher C–H stretching frequencies than solutions rich in the ionic liquid. This indicates that the $[\text{C}_2\text{mim}]^+$ cations participate in stronger hydrogen-bonding interactions when the triflic acid concentration is low, and the $[\text{C}_2\text{mim}]^+ \cdots \text{Tf}^-$ hydrogen bonds are gradually replaced by $\text{H}^+ \cdots \text{Tf}^-$ hydrogen bonds as the triflic acid content is increased. One way to view this situation is to consider the solutions as consisting of small $[\text{H}_n\text{Tf}_{n+1}]^-$ aggregate species, mediated by the imidazolium cations at intermediate compositions. In the high-concentration regime, hydrogen bonds between protons and triflate anions become the dominate species, promoting weaker hydrogen bonds between the imidazolium cations and the triflate anions.

5. Conclusions

Intense research efforts are focused on exploiting the favorable properties (i.e., high conductivities, low vapor pressures, and low flammabilities) of ionic liquids for lithium rechargeable batteries, fuel cells, and electrochemical capacitors. Understanding the molecular-level interactions between the ionic liquids and other compounds is a critical step toward developing these materials as electrolytes. In this work, the local structure of the $[\text{C}_2\text{mim}]^+$ and Tf^- ions is probed with infrared and Raman spectroscopy for a series of $[\text{C}_2\text{mim}]\text{Tf}-\text{HTf}$ solutions. Two vibrational modes of the triflate anion (viz., $\nu_s(\text{SO}_3)$ and $\delta_s(\text{CF}_3)$) are used to monitor the coordination environment of the anions in these systems. Frequency changes in these bands signal the presence of aggregated triflate anions. Spectroscopic features pointing toward the formation of an extended hydrogen-bonding network—similar to what would be expected in pure triflic acid—are observed in triflic acid-rich solutions. From another perspective, the addition of $[\text{C}_2\text{mim}]\text{Tf}$ to an HTf solution perturbs the extended hydrogen bonding present in the pure acid, leading to the formation of discrete, aggregated H–Tf species.

The vibrational modes of the $[\text{C}_2\text{mim}]^+$ cations are monitored to provide insight into the ion–ion interactions from the perspective of the cations. The Raman spectra suggest that the conformational equilibrium of the ethyl substituent is not affected by the addition of triflic acid. This is probably because the coordination sphere of the $[\text{C}_2\text{mim}]^+$ cations predominantly contains triflate anions, and both components in these solutions share the triflate anion. Thus, the addition of triflic acid does not significantly alter the contents of the immediate coordination shell of the imidazolium cation. There is spectroscopic evidence, however, that the addition of triflic acid does affect the hydrogen-bonding interactions between the cation and the triflate anions.

Acknowledgment. This work was funded by the U.S. Department of Defense, Army Research Office, under project number W911NF-04-1-0322.

References and Notes

- Hickner, M. A.; Ghassemi, H.; Kim, Y. S.; Einsla, B. R.; McGrath, J. E. *Chem. Rev.* **2004**, *104*, 4587.
- Song, Y.; Fenton, J. M.; Kunz, H. R.; Bonville, L. J.; Williams, M. V. *J. Electrochem. Soc.* **2005**, *152*, A539.
- Fuller, J.; Carlin, R. T. *Ionic Liquid-Polymer Impregnated Nafion Electrolytes In Molten Salts XII*; de Long, H. C.; Deki, S.; Stafford, G. R.; Trulove, P. C., Eds.; Electrochemical Society: Pennington, NJ, 1999; p 27.
- Navarra, M. A.; Panero, S.; Scrosati, B. *Electrochem. Solid-State Lett.* **2005**, *8*, A324.
- Sekhon, S. S.; Lalia, B. S.; Park, J.-S.; Kim, C.-S.; Yamada, K. *J. Mater. Chem.* **2006**, *16*, 2256.
- Doyle, M.; Choi, S. K.; Proulx, G. *J. Electrochem. Soc.* **2000**, *147*, 34.
- Nicolas, M.; Reich, R. *J. Phys. Chem.* **1979**, *83*, 749.
- Talaty, E. R.; Raja, S.; Storhaug, V. J.; Dölle, A.; Carper, W. R. *J. Phys. Chem. B* **2004**, *108*, 13177.
- Varetti, E. L. *Spectrochim. Acta* **1988**, *44A*, 733.
- Edwards, H. G. M. *Spectrochim. Acta* **1989**, *45A*, 715.
- Sampoli, M.; Marziano, N. C.; Tortato, C. *J. Phys. Chem.* **1989**, *93*, 7252.
- Umebayashi, Y.; Fujimori, T.; Sukizaki, T.; Asada, M.; Fujii, K.; Kanzaki, R.; Ishiguro, S.-I. *J. Phys. Chem. A* **2005**, *109*, 8976.
- Lassègues, J. C.; Grondin, J.; Holomb, R.; Johansson, P. *J. Raman Spectrosc.* **2007**, *38*, 551.
- Huang, W.; Frech, R.; Wheeler, R. A. *J. Phys. Chem.* **1994**, *98*, 100.
- Huang, W.; Wheeler, R. A.; Frech, R. *Spectrochim. Acta* **1994**, *50A*, 985.
- Rhodes, C. P.; Frech, R. *Macromolecules* **2001**, *34*, 2660.
- Sanders, R.; Frech, R.; Khan, M. A. *J. Phys. Chem. B* **2004**, *108*, 12729.

- (18) Sanders, R. A.; Frech, R.; Khan, M. A. *J. Phys. Chem. B* **2004**, *108*, 2186.
- (19) Sanders, R. A.; Frech, R.; Khan, M. A. *J. Phys. Chem. B* **2003**, *107*, 8310.
- (20) Burba, C. M.; Rocher, N. M.; Frech, R.; Powell, D. R. *J. Phys. Chem. B* **2008**, *112*, 2991.
- (21) Frech, R.; Huang, W. *J. Solution Chem.* **1994**, *23*, 469.
- (22) York, S. S.; Boesch, S. E.; Wheeler, R. A.; Frech, R. *Phys. Chem. Commun.* **2002**, *5*, 99.
- (23) Burba, C. M. *ECS Trans.* **2008**, *13*, 3.
- (24) Choudhury, A. R.; Winterton, N.; Steiner, A.; Cooper, A. I.; Johnson, K. A. *Cryst. Eng. Commun.* **2006**, *8*, 742.
- (25) Campbell, J. L. E.; Johnson, K. E.; Torkelson, J. R. *Inorg. Chem.* **1994**, *33*, 3340.
- (26) Bhargava, B. L.; Balasubramanian, S. *J. Phys. Chem. B* **2008**, *112*, 7566.
- (27) Huang, J.-F.; Chen, P.-Y.; Sun, I.-W.; Wang, S. P. *Spectrosc. Lett.* **2001**, *34*, 591.
- (28) Suarez, P. A. Z.; Einloft, S.; Dullius, J. E. L.; Dupont, J. *J. Chim. Phys.* **1998**, *95*, 1626.
- (29) Avent, A. G.; Chaloner, P. A.; Day, M. P.; Seddon, K. R.; Welton, T. *J. Chem. Soc., Dalton Trans.* **1994**, 3405.
- (30) Elaiwi, A.; Hitchcock, P. B.; Seddon, K. R.; Srinivasan, N.; Tan, Y.-M.; Welton, T.; Zora, J. A. *J. Chem. Soc., Dalton Trans.* **1995**, 3467.
- (31) Abdul-Sada, A. K.; Greenway, A. M.; Hitchcock, P. B.; Mohammed, T. J.; Seddon, K. R.; Zora, J. A. *J. Chem. Soc., Chem. Commun.* **1986**, 1753.
- (32) Fuller, J.; Carlin, R. T.; de Long, H. C.; Haworth, D. *J. Chem. Soc., Chem. Commun.* **1994**, 299.

JP902276B